Advances and Opportunities in the Design and Modeling of Vertical-Cavity Surface-Emitting Lasers

J. W. Scott, B. J. Thibeault, S. W. Corzine and L. A. Coldren
ECE Dept., University of California at Santa Barbara. Santa Barbara, California 93106

Abstract

The numerical models available for optoelectronic devices are quite limited. In the case of vertical cavity surface emitting lasers, almost no models have been developed. For the numerical modeler, this presents the opportunity to develop new insights but makes it difficult to determine which effects are dominant. Our group has maintained a very active program in vertical cavity lasers in which there has been a strong interaction between numerical modeling and experiment. Based on that experience, numerical simulations have been developed which predict the optical, electrical and current to light characteristics for index-guided vertical cavity lasers. This paper discusses the various physical effects we have modeled and points out the research areas which demand more involved calculations.

Vertical cavity lasers represent a relatively new class of semiconductor lasers. The development of epitaxially grown distributed Bragg reflectors with reflectivities in excess of 99% has enabled their realization in recent years. Interest in the lasers was originally based on their low divergence beams and potential for array applications. Initial experimental results showed low output powers and high drive voltages. Improvements have lead to low drive voltages, high differential efficiency, sub-milliamp thresholds and output powers well above 1 mW. More recently, it has been demonstrated that they can be designed to have temperature stabilized operation. The complex nature of the devices and the time and expense of fabrication cycles has driven the development of numerical models to aid the device design. Along with optical models to determine the electromagnetic fields, we have developed an LI simulator which includes thermal effects, carrier diffusion, stimulated emission and spatial hole burning[1].

Due to their small size and the distributed nature of the reflectors, many of the models used for conventional in-plane semiconductor lasers must be modified. The two lasers are contrasted in Fig. 1a. The low optical losses of the vertical cavity require accurate calculations. For example, additional

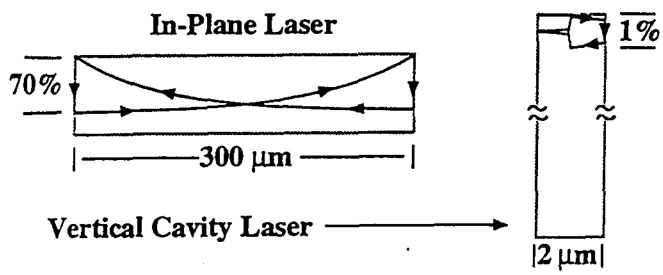

Fig 1a. Schematic comparing the optical power flow in an in-plane laser and a vertical cavity laser. The low losses of the high Q cavity requires accurate calculations

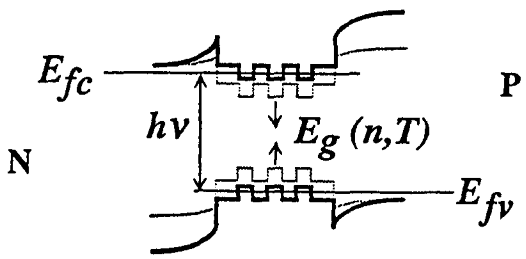

Fig 1b. Relationship of the cavity mode $h\nu$ and the band gap of the laser active region. The quasi-Fermi level separation is required to be greater than the photon energy.

round trip propagation losses of only 0.5% would reduce the optical efficiency nearly in half, resulting in a large reduction in the slope of the LI curve. The short cavity length results in a wide spacing of the Fabry-Perot modes, and thus only a single longitudinal mode falls within the optical gain spectrum of the quantum wells. As shown schematically in Fig. 1b, the bandgap shrinks toward lower energy (longer wavelengths) due to both ohmic heating and increasing carrier densities while the cavity mode, $h\nu$, essentially stays fixed. For lasing to occur, the necessary population inversion requires the quasi-Fermi level separation to be greater than the photon energy. At the optimum alignment of the cavity mode with the gain peak, the threshold current is at a minimum. Depending on their relative position at room temperature, a gain offset can be used to produce temperature stabilized operation. Once temperature rises have reduced the bandgap below the photon energy of the mode, carrier densities rise rapidly and carrier leakage can then become very important. Confirmation of these effects in three quantum well $In_{0.2}Ga_{0.8}As$ vertical cavity lasers has been reported in reference[2]. An earlier design of the 11μm diameter laser showed a threshold minimum near 35°C and a strong increase in carrier leakage over the $Al_{0.2}Ga_{0.8}As$ cladding layers at higher temperatures. Grown with a longer cavity and higher barrier $Al_{0.5}Ga_{0.5}As$ cladding layers, the newer design exhibited a minimum threshold current of 1.6 mA at 70°C with a variation of less than 0.5 mA over a 80°C range.

The small size of these lasers makes it possible to achieve very low threshold currents. At the same time, the small size makes surface effects very important. Even with the relatively low surface recombination velocities of these InGaAs wells, ~ 2 x 10^5 cm/s, surface recombination accounts for more than half of the threshold current for etched pillar, bottom emission designs. With improvements in the growth and fabrication technologies, new structures are being investigated. A schematic of an intra-cavity contacted laser[3] is shown in Fig. 2a. Both contacts to this top surface emitting laser are made using p and n doped layers within the optical cavity. A current constriction etch above the active layer is used to force the current into the optical mode, removing surface recombination from the region of current injection. The resulting LI characteristics are shown in Fig. 2b. The lasers have sub-milliamp thresholds with output powers well above 1 mW. Spatial hole

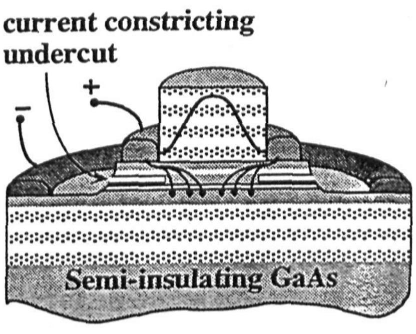

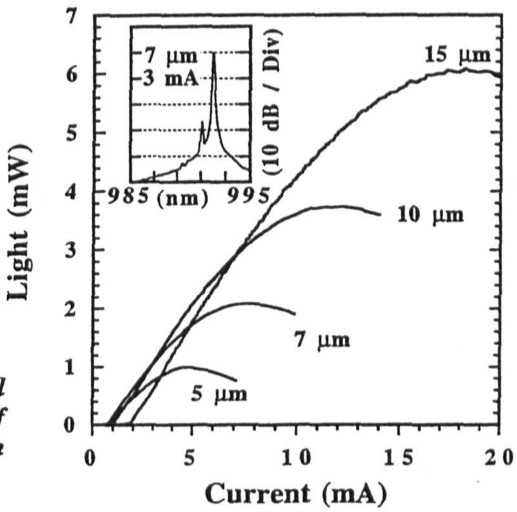

Fig. 2. Structure of an intra-cavity contacted vertical cavity laser and the measured LI characteristics of various diameters. The inset shows the optical spectrum of the 7 μm laser at 3 mA bias.

burning and surface scattering losses are competing effects, resulting in a wide variation in the transverse modal properties of the lasers depending on diameter. The 5 μm device lases in a single fundamental mode (MSR > 30 dB) while the 15 μm laser has four competing modes. The use of intra-cavity contacts allow both mirrors to be undoped, enabling microwave characterization using high speed probes and co-planer waveguides to make the transition from the probes to the lasers. To model these devices the following models have been developed.

I. Optical Model

The problem has been assumed to be separable into axial (growth direction) and transverse mode profiles. The transverse modes are calculated using the standard approach for determining the HE modes of a dielectric waveguide in cylindrical coordinates, using the averaged value for the index in the semiconductor. A transmission matrix approach is used to calculate the resonant cavity wavelength, threshold gain and optical losses for the axial fields. A transmission matrix is calculated for each layer in the cavity, and then they are multiplied together to find the transmission and reflection coefficients for the entire structure. To determine the lasing condition, a search is made in wavelength and gain to find the poles in reflectivity, so that light is emitted for no incoming field. The resulting gain is the threshold optical gain required for the particular design. Included in the formulation are complex dielectric constants, allowing the addition of optical gain or loss in any layer. It is important to use accurate models for the dispersion of the index for the various materials, in the AlGaAs system the data from Afromowitz[4] is often used. For the optical losses, the dominant losses are free carrier absorption. This plasma effect is modelled phenomenologically by using an absorption coefficient of $11cm^{-1}$ per $10^{18}cm^{-3}$ p-type carriers and $5cm^{-1}$ per $10^{18}cm^{-3}$ n-type carrier for a wavelength of 1 μm in GaAs. Very little data of the accuracy required exists in the literature. Proper calculation of this effect requires complex bandstructure models. It is important because resistance due to lower doping leads to heating which limits output power while higher doping leads to optical losses which reduce the output power. A balanced design requires more detailed knowledge of the tradeoffs.

To determine the optical efficiency, defined as the fraction of photons generated that are emitted out of the cavity, the threshold gain is calculated with and without optical losses. The ratio is the optical efficiency, typically between 50 and 70% for our designs. The transmission coefficient, T_r, can be calculated using the ratio of the field inside and outside the cavity. As shown schematically in Fig. 1, the round trip gain must compensate for the losses of transmission and internal loss. This is expressed as $G = L + T_r$ where the round trip gain G is related to the material gain g by:

$$G = 2g l_{act} \zeta_{enh} \tag{1}$$

where the two is for two passes (round trip), l_{act} is the total quantum well thickness and ζ_{enh} is the enhancement factor due to the standing wave effect. For our three 80Å quantum well design, ζ_{enh} has a value of 1.83 instead of the ideal 2 for an infinitely thin layer placed at the antinode. A final note is that the inclusion of diffraction losses requires complete 3D solutions, a much more complex problem given the relatively large index discontinuities at each interface of the distributed Bragg reflectors. Furthermore, gain-guided structures pose an even more complex problem. The transverse modes are dominated by the weak index guide generated by the thermal gradients associated with the current flow, and thus the thermal, electrical and optical properties must be solved self consistently in 3D. We restrict ourselves here to strongly index-guided structures. An additional point is that the local temperature may need to be included in the calculation as the bandgaps (and hence indices of refraction) of the various layers shift at different rates relative to the lasing wavelength resulting in a changing transmission coefficient for the mirror. While we have not yet included this effect, others have reported[5] on significant reductions in the transmission coefficient at elevated temperatures.

II. Gain Model

The gain model for vertical cavity lasers must provide the material gain as a function of carrier density, temperature and wavelength. Due to the small size of the lasers, their thermal impedance is high, and typically junction temperature rises as the output "rolls over" are above 100°C. In addition, carrier densities exceed $10^{19}cm^{-3}$ due to spatial hole burning and bandgap shifts from heating. The position of the cavity mode shifts due to index dispersion at a rate of ≈0.8Å/°C while the bandgap shifts at ≈3.4Å/°C. Thus the gain spectrum must be known as well since the gain peak shifts its relative position during laser operation. To determine the gain spectrum, we use a first principle gain model that includes valance band mixing and the effects of strain[6]. Typical output is shown in Fig. 3. It has proved to be critical to include the band shrinkage effect in order to explain the threshold characteristics observed as a function of temperature. This has been included using the phenomenological formula $\Delta E_g = -Cn^{1/3}$ and can be seen as the shift of the band edge towards longer wavelengths with increasing carrier densities in Fig. 3a. Finally, the gain model also provides the spontaneous emission as a function of carrier density. This is calculated using the band structure, the matrix elements, and assuming a virtual photon in each radiation mode. As can be seen in Fig. 3b, it is inappropriate to assume a linear relationship for the peak gain as a function of carrier density. For the following models, either curve fits or lookup tables for the gain data shown in Fig. 3 have been used to speed the calculations.

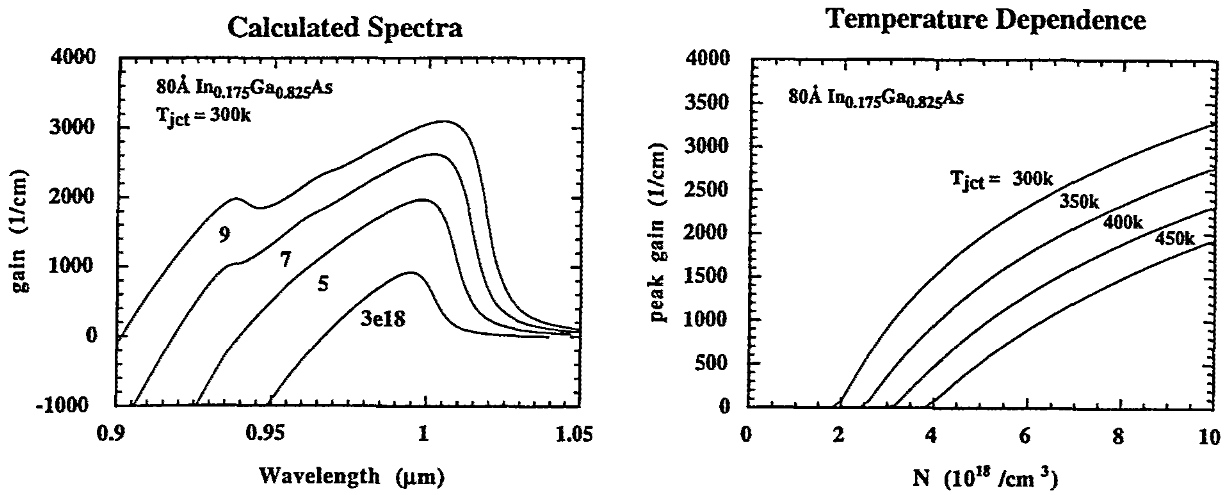

Fig. 3 Calculated gain spectra and peak gain for the strained InGaAs quantum wells

III. LI Model

The current to light (LI) model is shown schematically in Fig. 4a. The carrier density profile is solved self consistently in cylindrical coordinates. The radial ambipolar diffusion currents, stimulated emission, spontaneous emission, Auger recombination, surface recombination and carrier leakage currents are balanced in each cell. Input parameters include the transverse mode profile, the injected current density profile for each voltage, the cavity mode shift with temperature, and an effective thermal conductivity. The temperature rise is assumed constant across the junction and calculated using the analytic formula for a disc on a semi-infinite substrate[7]:

$$\Delta T_{jct} = 1/4 r_{act} k_{sub} \qquad (2)$$

where ΔT_{jct} is the junction temperature rise, r_{act} is the active region radius and k_{sub} is the effective thermal conductivity. Note that the thermal conductivity of the ternary and quaternary materials can be 10-20 times higher than the binaries such as GaAs due to random alloy scattering of phonons. The simple etched pillar structures that we fabricate make the analytic approximation reasonable. Fully buried structures such as the proton implanted gain-guided designs require numerical calculation. Complete continuous wave (CW) LI characteristics are calculated using this approach. Most of our calculations assume a single transverse mode for simplicity, however, the calculations can be run with multiple transverse modes at the expense of slower convergence.

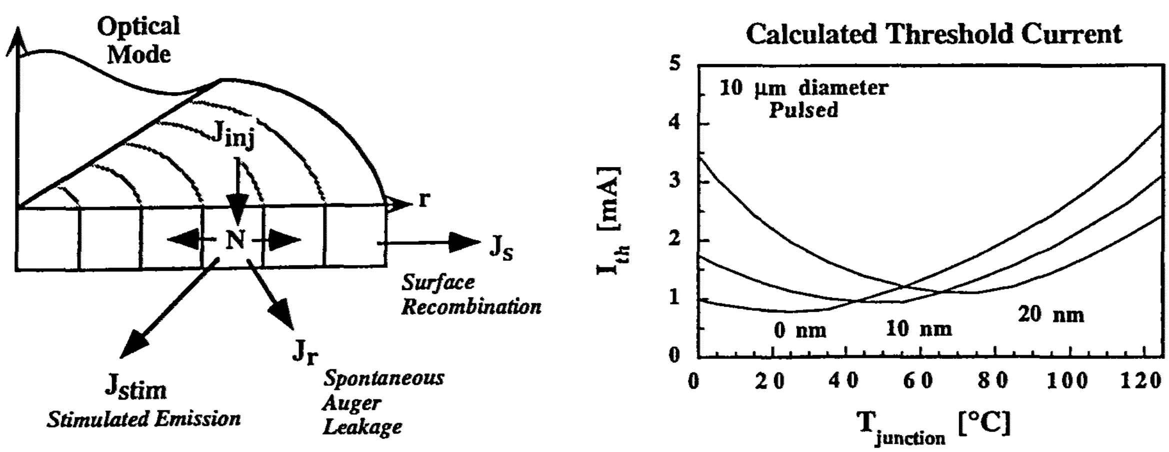

Fig. 4. Schematic of the LI model and a simulation of the threshold current for varying gain offsets

Results of a calculation with the LI model for determining the threshold current under pulsed operation ($\Delta T_{jct} = 0$) are shown in Fig. 4b. Several different curves are shown, corresponding to varying offsets of the cavity mode and the gain peak. The calculation used an ambipolar diffusion constant of 20cm^2/s and a surface recombination velocity of 2x10^5 cm/s. This temperature insensitive operation is radically different from the behavior of in-plane lasers, whose threshold current always increases with increasing temperature. The reduced threshold with increasing temperature is a result of the interplay of the band shrinkage effect and the spectral gain curve while the increase in threshold at elevated temperatures is primarily due to Auger recombination. The coefficient used for our calculations of these InGaAs quantum wells has been fit to the data using the typical $C_A n^3$ dependence with an Auger coefficient C_A =1x10^{-29} cm^6/s, three times higher than bulk GaAs. It is interesting that bandgap renormalization and Auger recombination play a dominant role in these lasers, typically they are second order effects for in-plane lasers in the GaAs system. As researchers attempt to make vertical cavity lasers at other wavelengths, accurate models for these effects will become more important. In particular, Auger recombination at high carrier densities can be reduced by modifying the bandstructure with strain. This will be very important in the telecommunication wavelengths and requires much more complex numerical calculations.

IV. Current Injection

For top emitting laser structures or those using dielectric distributed Bragg reflectors, ring contacts such as those shown in Fig. 1 are inevitable. The concern is that current crowding will occur at the periphery of the laser where the fundamental optical mode is weak. The result will be reduced internal efficiency and the tendency to promote multimode operation by enhancing the gain near the perimeter. We have taken care to model the current injection for our intra-cavity contacted designs. Accurate models for the JV characteristics of the p-i-n and heterojunctions are required as it is the differential resistance which determines the distribution of current once the diodes have been forward biased. Particularly in Be doped AlGaAs, the dopants can diffuse during growth resulting in unknown dopant profiles. To model our diodes we have grown test active regions and measured their JV characteristics under uniform injection conditions. The measured characteristics are used in the simulation. To calculate the injected current density as a function of radius the laser is divided into a mesh in cylindrical coordinates as shown in Fig. 5a where the nonlinear materials are lightly shaded. The voltage and current distribution is found using an Alternating Direction Iteration (ADI) technique where the diodes have been linearized. The diode resistance values are adjusted during the iteration process so that the final solution uses the correct JV characteristics. The results of such a calculation are shown in Fig. 5b. For this particular doping, diodes and geometry, the current flowing through the p-i-n junction shows current crowding at the edge only above 6 mA of drive current. Since the threshold current for this laser is below 1 mA, this is an acceptable design.

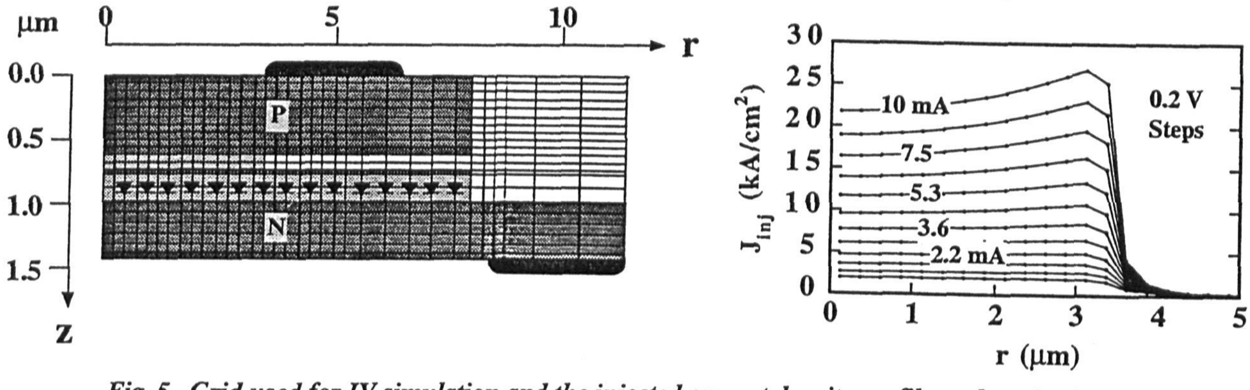

Fig. 5. Grid used for IV simulation and the injected current density profile at the p-i-n junction

V. Intra-Cavity Laser Simulation

Combining the output of the current injection calculations with the LI simulation gives a complete current, voltage, light characteristic simulation of the intra-cavity contacted devices of Fig. 2. The results of such a calculation are shown in Fig. 6a for the 7 μm diameter laser. With all input variable determined by the model for the uniformly injected lasers, the only parameter adjusted for fitting was the gain offset. Spectral measurements and room temperature photoluminescence of the active material had indicated a gain offset on the order of 10 nm, in good agreement with the chosen gain offset of 5nm. The calculated carrier density profiles are shown in Fig. 6b. Two important points can be determined from the plot. First, that the effects of surface recombination have been greatly

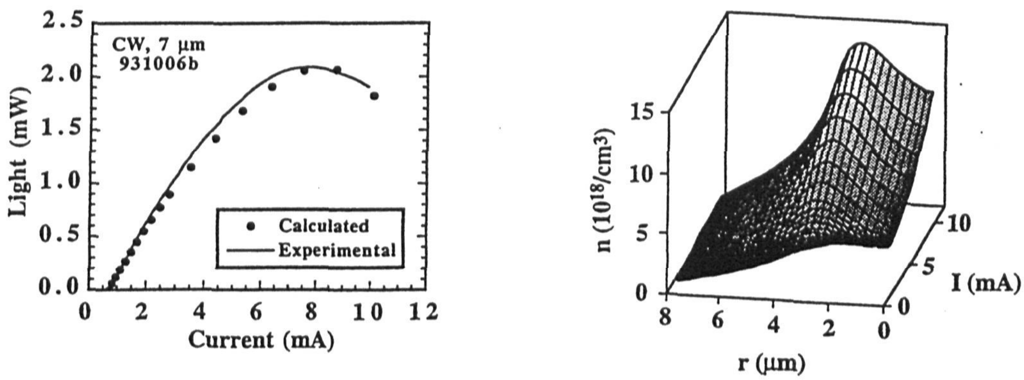

Fig. 6. Comparison of calculated and experimental LI characteristics for the 7µm intra-cavity laser of Fig. 2. The radial carrier density profile for varying bias currents is shown on the right.

reduced by this current constricted design. Second, that there is a large inefficiency resulting from the carriers injected at the edge of the optical waveguide where the optical mode is weak. If, instead, the current constriction could be made to a diameter less than the transverse mode diameter, greater internal efficiency would be observed while the single mode operation would be enhanced. These more difficult "gain apertured" designs are currently under investigation in our lab and others.

VI. Conclusion

Models for the optical,electrical and LI characteristics of vertical cavity lasers have been presented to demonstrate the current state of the laser simulation and to point out the dominant device physics. While agreement with experiment is good, most of the approximations have been made possible by restricting our analysis to strongly index guided structures. As research begins to focus on designs which combine the features of the index guided and gain guided structures, fully self consistent solutions of the current, thermal and optical problems will be required. In addition, many important physical effects have been included using phenomenological models. The high optical gain requirements of the short vertical cavity pose challenges to develop efficient vertical cavity lasers at shorter and longer wavelengths. Comprehensive models of free carrier absorption, Auger recombination and band gap renormalization in strained and unstrained materials may provide insights into better designs for these more challenging material systems. This work was sponsored by ARPA via the Optoelectronics Technology Center.

References

[1] J. W. Scott, R. S. Geels, S. W. Corzine and L. A. Coldren, " Modeling temperature effects and spatial hole burning to optimize vertical cavity surface emitting laser performance" *IEEE J. Quantum Electron.*, **29** (5) (1993)

[2] J. W. Scott, D. B. Young, S. W. Corzine and L. A. Coldren, " Modeling the current to light characteristics in index guided vertical-cavity surface-emitting lasers," *Appl Phys Lett.*, **62** (10) pp1050-1052 (1993)

[3] J. W. Scott, B. J. Thibeault, D. B. Young and L. A. Coldren, "High Efficiency Sub-Milliamp Vertical Cavity Lasers with Intra-Cavity Contacts" *IEEE Photonics Tech. Lett.*, **6** (6), (1994)

[4] M. A. Afromowitz, "Refractive index of $Ga_{1-x}Al_xAs$," *Solid State Comm.*, **15**, (59) (1974)

[5] J. Piprek, H. Wenzel and G Sztefka, "Modeling Thermal Effects on the Light vs Current Characteristic of Gain-Guided Vertical-Cavity Surface-Emitting Lasers," *IEEE Photonics Tech. Lett.*, **6** (2), pp 139-142 (1994)

[6] S. W. Corzine, R. H. Yan and L. A. Coldren, "Theoretical Gain in Strained InGaAs/AlGaAs Quantum Wells, Including Valence Band-Mixing Effects," *Appl. Phys. Lett.*, 57 (27) pp 2835-2837 (1990)

[7] S. S. Kutateladze, V. M. Borishanskii, *A Concise Encyclopedia of Heat Transfer*, Oxford: Permagon,1966, p43